第 43 卷 第 17 期/2023 年 9 月/光学学报 特邀论文

光学学报

基于飞秒激光刻写的高功率啁啾倾斜光纤光栅

李昊[1,2]，叶新宇[1,2]，王蒙[1,2,3*]，武柏屹[1,2,3]，高晨晖[1,2]，陈子伦[1,2,3]，王泽锋[1,2,3**]，陈金宝[1,2,3]

[1]国防科技大学前沿交叉学科学院，湖南 长沙 410073；

[2]国防科技大学南湖之光实验室，湖南 长沙 410073；

[3]国防科技大学高能激光技术湖南省重点实验室，湖南 长沙 410073

摘要 啁啾倾斜光纤光栅(CTFBG)是高功率光纤激光中抑制受激拉曼散射(SRS)的核心器件，极具应用价值与研究前景。然而，传统紫外激光制备的CTFBG难以承受较高功率，限制了其发展与应用。本文基于飞秒激光的相位掩模板法在20/400 μm大模场双包层光纤中分别刻写了光纤布拉格光栅(FBG)对与CTFBG。使用FBG对搭建了高功率光纤振荡器，并将CTFBG置于振荡器的谐振腔内抑制SRS。结果表明，CTFBG最大承受功率为2.8 kW，最大拉曼抑制比为～13 dB，插损小于2%，功率温升系数为7.8 ℃/kW。本文验证了飞秒激光刻写的CTFBG具有优异的功率承受能力，将进一步推动高功率光纤激光技术的发展。

关键词 飞秒激光；光纤激光器；受激拉曼散射；光纤光栅；啁啾倾斜光纤光栅

中图分类号 TN248 **文献标志码** A **DOI**：10.3788/AOS230946

1 引 言

高功率光纤激光器具有结构紧凑稳定、转换效率高、光束质量好、可柔性操作等优点，在工业加工、生物医疗等领域具有重要的应用价值[1]。随着高功率光纤激光器的输出功率不断提高，受激拉曼散射(SRS)等非线性效应成为了制约其性能提升的主要因素。目前主要有以下几种方法被用于抑制高功率激光系统中的SRS，包括增大光纤面积[2]、使用光谱选择光纤[3]、使用长周期光纤光栅(LPFG)[4-5]或啁啾倾斜光纤光栅(CTFBG)[6-14]作为光谱滤波器件等。与其他方法相比，使用LPFG与CTFBG抑制SRS具有制作方便、操作简单的优点，受到更广泛的研究与应用。然而，LPFG对温度、应力等外界因素较为敏感，其光谱特性相对不稳定，影响其滤除效果。CTFBG则具有更好的光谱稳定性，目前已被用于数千瓦量级的光纤激光器中抑制SRS，并且成功实现了商业化[15-16]，极具应用价值与研究前景。传统的CTFBG制备方法是紫外激光相位掩模板法[6]，在刻写光栅前后要对光纤进行载氢与退火处理。这不仅导致CTFBG的制备周期较长，并且当退火处理不彻底时，光栅中残留的氢分子和羟基化合物会吸收激光发热[7]，从而限制CTFBG的功率承受能力。因此，大多数报道都是将CTFBG应用在光纤放大器的种子与放大级之间抑制SRS[6,8-10,14]，难以将其应用在光纤振荡器谐振腔内等需要承受较高功率的场景[12-13]。目前CTFBG只应用在最高2.03 kW的光纤振荡器谐振腔内抑制SRS[13]，这无疑限制了CTFBG的应用与发展。为了研制高功率CTFBG，研究人员提出了新型退火方法[7]、分布式刻写技术[11]以及使用高效制冷封装夹具[17]来改善CTFBG的功率温升特性，从而提高其功率承受能力。然而，这些方法都大大增加了高功率CTFBG的制备周期、工艺复杂程度和经济成本。目前为止，刻写在25/400 μm大模场光纤的高功率CTFBG传输功率已突破4 kW[17]；刻写在芯径20 /400 μm大模场光纤中的商用高功率CTFBG产品，其功率承受能力指标一般是3 kW量级[15-16]。

随着飞秒激光刻写技术的发展[18-20]，为研制高功率CTFBG提供了新的思路。飞秒激光对光纤光敏性没有要求，所以光纤无需载氢和退火处理，这既缩短了光纤布拉格光栅(FBG)的制备周期，也避免了退火不彻底引起的吸收发热。此外，飞秒激光刻写的FBG还具有耐高温的优点，对激光引起的温升也具有更好的鲁棒性，可以在高温下稳定工作。目前，基于飞秒激光刻写的FBG对已经实现了高功率全光纤激光振荡器[21-26]，最大输出功率达到8 kW[23,26]，证明了飞秒激光刻写的FBG具有良好的功率承受能力。近期，本课题组首次

收稿日期：2023-05-08；**修回日期**：2023-06-04；**录用日期**：2023-06-16；**网络首发日期**：2023-07-31

基金项目：国家自然科学基金(11974427，12004431)、湖南省科技创新计划(2021RC4027)、脉冲功率激光技术国家重点实验室项目(SKL2020ZR05，SKL2021ZR01)

通信作者：*gfkdqy@163.com；**zefengwang_nudt@163.com

报道了基于飞秒激光刻写的CTFBG[27-28]，并应用在千瓦量级光纤激光器的输出端进行拉曼滤除实验[29]。然而，飞秒激光刻写的CTFBG还未应用在光纤振荡器的谐振腔内抑制SRS，并且其功率承受能力也需要进一步研究。

本文基于飞秒激光相位掩模板法在20/400 μm大模场双包层光纤中分别刻写了FBG对与CTFBG。FBG对的中心波长为1080 nm，CTFBG的中心波长为1133 nm，对应1080 nm信号光产生的拉曼光波长。使用FBG对搭建了高功率光纤振荡器，并将CTFBG插入振荡器的谐振腔内抑制SRS，振荡器的输出功率从2678 W提高至2811 W，光束质量M^2因子从1.54优化至1.43。CTFBG最大拉曼抑制比为~13 dB，插损小于2%，其在风冷条件下的功率温升系数为7.8 ℃/kW，远小于同等制冷条件下的紫外激光刻写的CTFBG功率温升系数。实验结果表明，飞秒激光刻写的CTFBG具有良好的功率承受能力与SRS抑制效果。

2　实验系统

2.1　FBG和CTFBG的制备

基于飞秒激光相位掩模板法分别制备了FBG对与CTFBG，刻写装置与文献[26，28]中基本相同。光源输出波长为515 nm的准直飞秒激光，飞秒激光经过反射镜组反射后，正入射柱面镜和线性啁啾相位掩模板，最终聚焦于待刻写的20/400 μm大模场双包层光纤纤芯内。使用飞秒激光振镜扫描技术[26]或倾斜扫描技术[28]在光纤中刻写腔镜用FBG或CTFBG。图1(a)和1(b)分别展示了测量得到的高反FBG(HRFBG)与低反FBG(LRFBG)光谱，两者的中心波长都为1080 nm。HRFBG的透射谱深度大于20 dB，反射率大于99%，反射谱的3 dB带宽约为3.6 nm。LRFBG的透射谱深度约为0.5 dB，反射率约为10%，反射谱的3 dB带宽约为1.2 nm。使用飞秒激光刻写的CTFBG光谱如图2所示，在刻写过程中采用了级联刻写技术来增大CTFBG的透射谱带宽[29]。CTFBG的透射谱带宽为17.3 nm，深度大于20 dB，透射谱中心波长为1133 nm，与1080 nm信号光对应的一阶拉曼光波长相匹配。使用波长1080 nm光纤激光器与功率计通过截断法测量CTFBG的损耗小于2%。

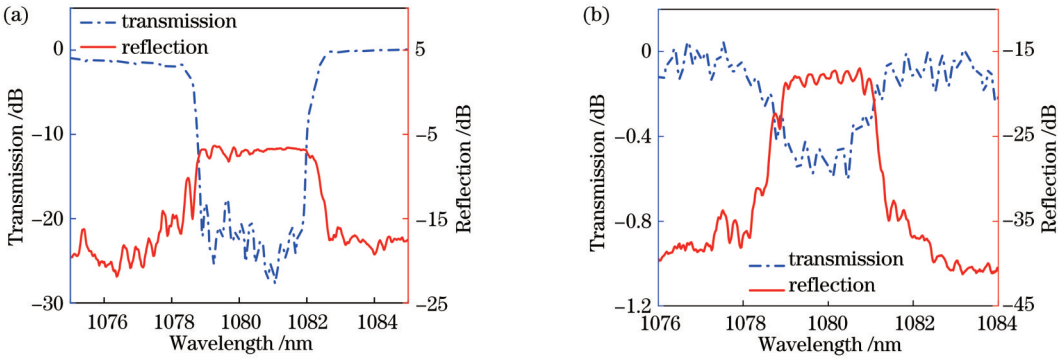

图1　飞秒激光刻写的FBG对的光谱。(a)高反FBG；(b)低反FBG

Fig. 1　Spectra of FBG pair written by femtosecond laser. (a) HRFBG; (b) LRFBG

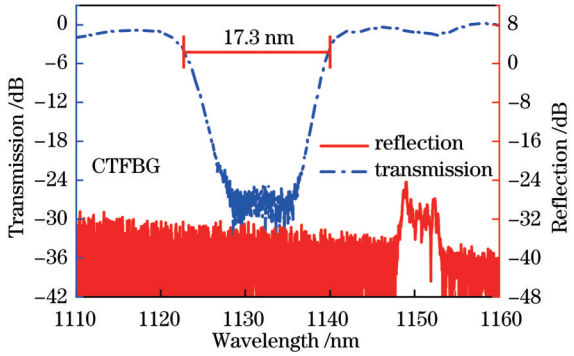

图2　飞秒激光刻写的CTFBG的光谱

Fig. 2　Spectrum of CTFBG written by femtosecond laser

2.2　高功率光纤振荡器测试系统

使用自研的FBG对搭建高功率光纤振荡器用于测试CTFBG，测试系统如图3所示。20/400 μm大模场双包层掺镱光纤(YDF)的长度为20 m，YDF两端与光纤合束器的输入信号纤熔接，合束器的输出信号纤与腔镜用FBG熔接。振荡器的泵浦方式为双向泵浦，泵浦源为976 nm的稳波长半导体激光器(LD)。正向输出激光经过包层光滤除器(CLS)后，通过光纤准直器(QBH)输出。振荡器的反向输出端切斜角以避免端面反馈。CTFBG插入后，截短相同长度的无源光纤以保证合束器和LRFBG之间的光纤长度不变，测试系统其余部分保持不变。

3　实验结果与分析

图4(a)和4(b)分别展示了插入CTFBG前后，不同泵浦功率下的输出光谱。在CTFBG插入前，当泵浦功率为3703 W时输出光谱中观察到了拉曼光成分，而当CTFBG插入后拉曼光成分几乎被完全滤除。当

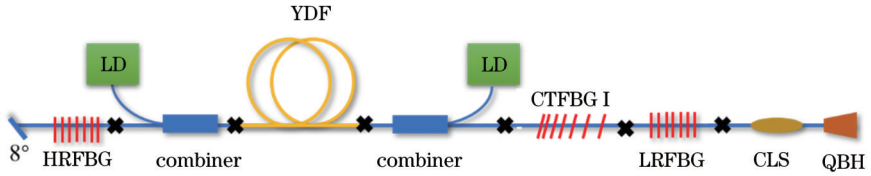

图 3 基于高功率光纤振荡器的CTFBG测试系统

Fig. 3 CTFBG testing system based on high-power fiber oscillator

泵浦功率增大到3842 W后，拉曼光谱线的宽度也随之增大，未插入CTFBG时的信号光与拉曼光的强度之比为～40 dB。当CTFBG插入后，由于CTFBG的滤除带宽有限，还有部分拉曼光未被滤除，信号光与拉曼光的强度之比只增大到～46 dB，如图4(c)所示。为了更清晰地展示CTFBG的滤除效果，将图4(c)中的两个光谱相减，可以得到CTFBG的拉曼抑制谱，如图4(d)所示。图中虚线为拟合曲线，CTFBG的拉曼抑制比最大为～13 dB。

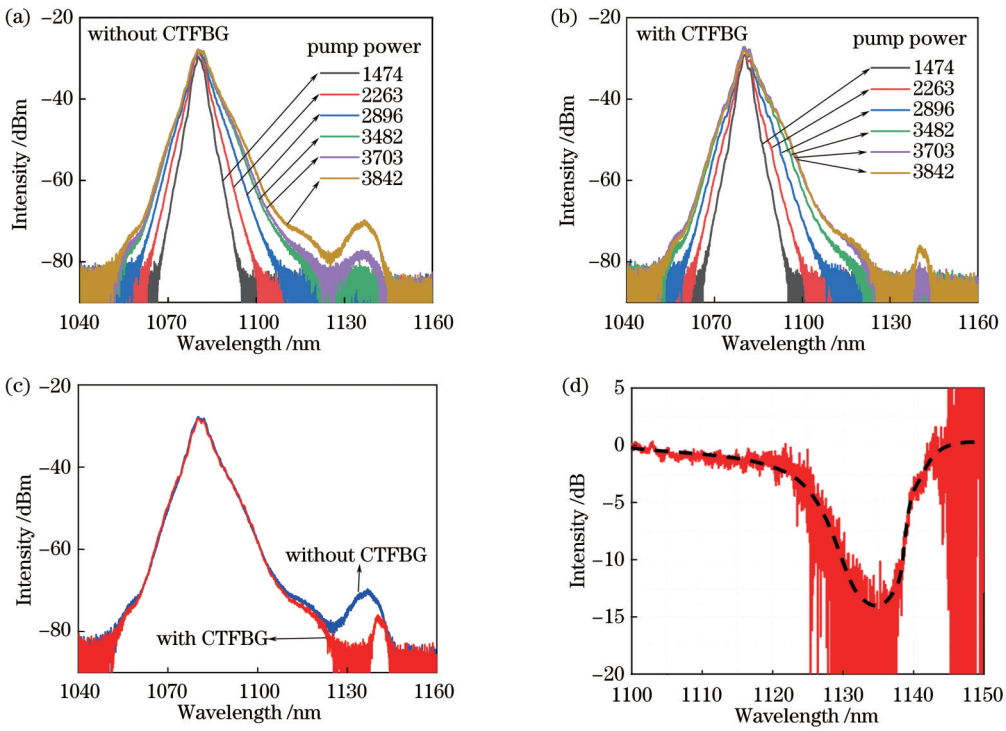

图 4 输出光谱实验结果。(a)未加CTFBG与(b)加入CTFBG时，不同泵浦功率下的输出光谱；(c)最大功率下的输出光谱对比；(d)CTFBG的拉曼抑制谱

Fig. 4 Output spectral experimental results. Output spectra at different pump powers (a) without and (b) with CTFBG; (c) comparison of output spectra at maximum power; (d) Raman suppression spectrum of CTFBG

图5(a)展示了CTFBG插入前后振荡器的输出功率变化曲线，以及最高功率下的输出光斑形态。同时，为了更清晰地对比输出功率的变化，将图5(a)中的虚线框部分进行局部放大，如图5(b)所示。未插入CTFBG时，当泵浦功率大于3500 W后，振荡器效率下降。最大泵浦功率下的输出功率为2678 W，光光转换效率为69.7%，光束质量M^2因子为1.54。将CTFBG插入谐振腔后，由于其具有小于2%的插损，激光器的输出功率略微下降。然而，当泵浦功率增大至3500 W之后，振荡器效率未出现下降现象，在最大泵浦功率下的输出功率提高到2811 W，光光转换效率为73.2%。振荡器输出光束质量也有所优化，M^2因子减小为1.43。为了进一步确定CTFBG插入前后，高功率下振荡器效率变化的原因，对输出激光的时域信号进行测量。图5(c)展示了CTFBG插入前的时域信号，插图为时域信号对应的傅里叶频谱。尽管图5(c)中的时域信号并未出现明显的周期性波动，但是在其傅里叶频谱上可以观察到较显著的频率峰，表明此时出现了横向模式不稳定(TMI)现象[30]。而此时光谱中的拉曼光强度较弱，低于信号光强度～40 dB[见图4(a)]。因此，SRS对振荡器效率的影响较弱，造成振荡器效率下降的主要原因是TMI。图5(d)展示了CTFBG插入后的时域信号与对应的傅里叶频谱。当CTFBG插入后，傅里叶频谱中的频率峰消失，表明未

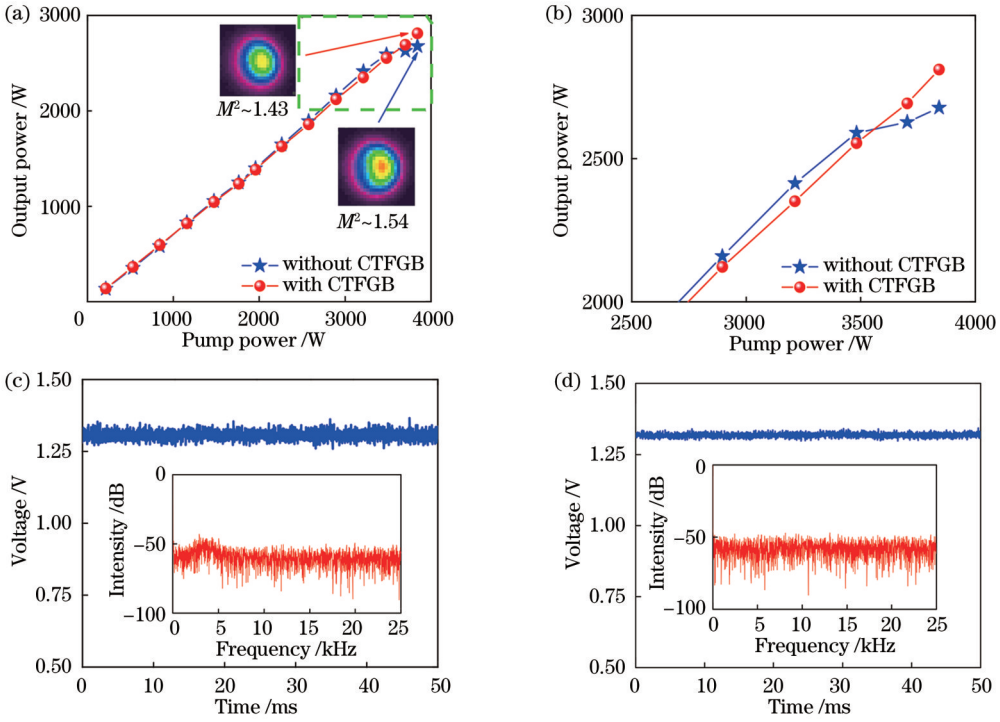

图 5　输出功率与时域信号实验结果。(a)输出功率变化曲线，插图为输出光斑形态；(b)局部放大的输出功率变化曲线；(c)未加CTFBG与(d)加入CTFBG时，输出激光的时域信号，插图为对应的傅里叶频谱

Fig. 5　Experimental results of output power and time domain signal. (a) Output power variation curve, and insert is profile of output laser beam; (b) output power variation curve of local zooming; time domain signal of output laser (c) without and (d) with CTFBG, and insert is corresponding Fourier spectrum

出现TMI现象。因此，CTFBG插入后不仅抑制了SRS，也抑制了TMI的产生。这是因为SRS会诱导纤芯基模到高阶模的转换，从而降低TMI的阈值，所以当SRS被抑制后，TMI阈值也会有所提高[31]。由于TMI还会引起光束质量退化，所以在TMI未产生后光束质量M^2因子从1.54减小至1.43，这意味着CTFBG插入后还使光束质量得到优化。

在测试过程中，CTFBG未封装，而是将其悬空并使用风扇制冷，以方便使用红外热像仪准确测量温度。图6(a)展示了CTFBG随光纤振荡器输出功率的变化，虚线为实测数据的线性拟合。风冷条件下，CTFBG功率温升系数为7.9 ℃/kW。相比之下，使用紫外激光在大模场双包层光纤中刻写的CTFBG，其退火后在风冷条件下的功率温升系数通常都在15 ℃/kW以上[7,11]。因此，飞秒激光刻写的CTFBG的功率温升系数远小于同等制冷条件下的紫外激光刻写的CTFBG，表明飞秒激光刻写的CTFBG具有良好的功率温升特性。图6(b)为最高输出功率下的CTFBG热像图，CTFBG的栅区温度为44 ℃，还处在安全稳定的工作温度。因此，CTFBG的功率承受水平只是受

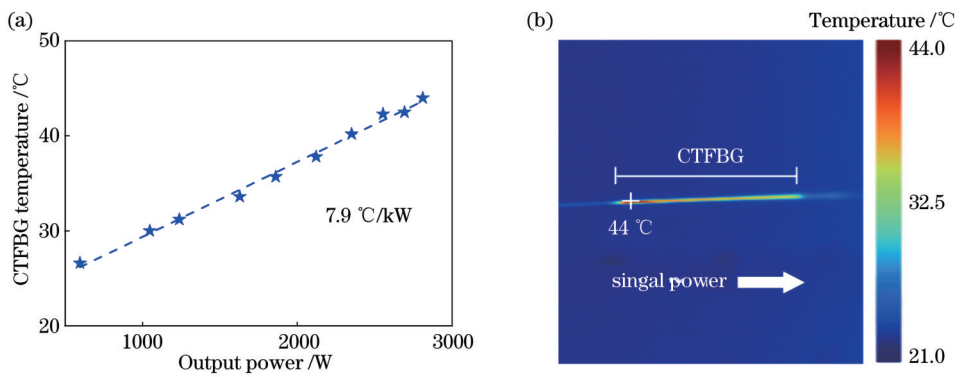

图 6　CTFBG温度特性实验结果。(a) CTFBG的温度随输出功率的变化；(b)最高输出功率下CTFBG的热像图

Fig. 6　Experimental results of CTFBG temperature characteristics. (a) CTFBG temperature as function of output power; (b) CTFBG thermography at maximum output power

限于光纤振荡器本身功率，还有进一步提高的潜力。

4 结 论

本文验证了飞秒激光刻写的CTFBG具有良好的功率承受能力与SRS抑制效果。使用飞秒激光在大模场双包层光纤中分别刻写了波长为1080 nm的FBG对与波长为1133 nm的CTFBG。使用FBG对搭建了高功率光纤振荡器，并将CTFBG插入振荡器的谐振腔内抑制SRS后，振荡器的输出功率从2678 W提升至2811 W，提升了5%，并且光束质量也得到优化，M^2因子从1.54减小至1.43。CTFBG最大拉曼抑制比为~13 dB，插损小于2%，最高温度为44 ℃。实验结果表明，飞秒激光在刻写高功率CTFBG方面具有很大的潜力，飞秒激光研制的高功率CTFBG性能已经媲美传统紫外激光刻写的CTFBG。本工作中，CTFBG的功率承受提升受限于振荡器本身功率，还有进一步提高的空间。今后通过优化飞秒激光刻写工艺，可以实现在更大芯径的光纤中不剥除涂覆层刻写CTFBG，并结合高效制冷封装夹具，有望研制万瓦量级承受功率的CTFBG。此外，还可以使用飞秒激光在直接有源光纤中刻写高功率CTFBG抑制SRS，这将有利于提高光纤激光系统的紧凑性。

参 考 文 献

[1] 周朴，冷进勇，肖虎，等. 高平均功率光纤激光的研究进展与发展趋势[J]. 中国激光，2021，48(20)：2000001.
Zhou P，Leng J Y，Xiao H，et al. High average power fiber lasers：research progress and future prospect[J]. Chinese Journal of Lasers，2021，48(20)：2000001.

[2] Wang Y，Xu C Q，Po H. Analysis of Raman and thermal effects in kilowatt fiber lasers[J]. Optics Communications，2004，242(4/5/6)：487-502.

[3] Zenteno L，Wang J，Walton D，et al. Suppression of Raman gain in single-transverse-mode dual-hole-assisted fiber[J]. Optics Express，2005，13(22)：8921-8926.

[4] Jiao K R，Shen H，Guan Z W，et al. Suppressing stimulated Raman scattering in kW-level continuous-wave MOPA fiber laser based on long-period fiber gratings[J]. Optics Express，2020，28(5)：6048-6063.

[5] Hu Q H，Zhao X F，Tian X，et al. Raman suppression in 5 kW fiber amplifier using long period fiber grating fabricated by CO_2 laser[J]. Optics & Laser Technology，2022，145：107484.

[6] Wang M，Zhang Y J，Wang Z F，et al. Fabrication of chirped and tilted fiber Bragg gratings and suppression of stimulated Raman scattering in fiber amplifiers[J]. Optics Express，2017，25(2)：1529-1534.

[7] Jiao K R，Shu J A，Shen H A，et al. Fabrication of kW-level chirped and tilted fiber Bragg gratings and filtering of stimulated Raman scattering in high-power CW oscillators[J]. High Power Laser Science and Engineering，2019，7(2)：e31.

[8] Wang M，Liu L，Wang Z F，et al. Mitigation of stimulated Raman scattering in kilowatt-level diode-pumped fiber amplifiers with chirped and tilted fiber Bragg gratings[J]. High Power Laser Science and Engineering，2019，7(1)：e18.

[9] Wang M，Wang Z F，Liu L，et al. Effective suppression of stimulated Raman scattering in half 10 kW tandem pumping fiber lasers using chirped and tilted fiber Bragg gratings[J]. Photonics Research，2019，7(2)：167-171.

[10] Tian X，Zhao X F，Wang M，et al. Influence of Bragg reflection of chirped tilted fiber Bragg grating on Raman suppression in high-power tandem pumping fiber amplifiers[J]. Optics Express，2020，28(13)：19508-19517.

[11] Song H Q，Yan D L，Wu W J，et al. SRS suppression in multi-kW fiber lasers with a multiplexed CTFBG[J]. Optics Express，2021，29(13)：20535-20544.

[12] Lin W X，Desjardins-Carrière M，Sévigny B，et al. Raman suppression within the gain fiber of high-power fiber lasers[J]. Applied Optics，2020，59(31)：9660-9666.

[13] Lin W X，Desjardins-Carrière M，Iezzi V L，et al. Simple design of Yb-doped fiber laser with an output power of 2 kW[J]. Optics & Laser Technology，2022，156：108448.

[14] Zhao X F，Tian X，Wang M，et al. Design and fabrication of wideband chirped tilted fiber Bragg gratings[J]. Optics & Laser Technology，2022，148：107790.

[15] Raysung Photonics company. Product introduction on the chirped and tilted fiber Bragg gratings as the Raman Scattering Suppressor[EB/OL]. [2023-02-3]. https://www.raysung.com/html/Raman_scattering_suppressor/index.html.

[16] Advanced Fiber Resources company. Product introduction on the chirped and tilted fiber Bragg gratings as the Raman Scattering Suppressor[EB/OL]. [2023-02-3]. https://www.fiber-resources.com/clearcut-raman-scattering-suppression-fbg_p659.html.

[17] 王蒙，田鑫，赵晓帆，等. 国产25 μm/400 μm啁啾倾斜光纤光栅传输功率突破4 kW[J]. 中国激光，2022，49(6)：0615001.
Wang M，Tian X，Zhao X F，et al. Transmission power of homemade chirped and tilted fiber Bragg grating on 25 μm/400 μm fiber exceeding 4 kW[J]. Chinese Journal of Lasers，2022，49(6)：0615001.

[18] 廖常锐，何俊，王义平. 飞秒激光制备光纤布拉格光栅高温传感器研究[J]. 光学学报，2018，38(3)：0328009.
Liao C R，He J，Wang Y P. Studyon high temperature sensors based on fiber Bragg gratings fabricated by femtosecond laser[J]. Acta Optica Sinica，2018，38(3)：0328009.

[19] 李宏业，饶斌裕，赵晓帆，等. 基于飞秒激光刻写光纤光栅的研究进展[J]. 激光与光电子学进展，2020，57(11)：111420.
Li H Y，Rao B Y，Zhao X F，et al. Development of fiber gratings inscribed by femtosecond laser[J]. Laser & Optoelectronics Progress，2020，57(11)：111420.

[20] 吕瑞东，陈涛，范春松，等. 飞秒激光制备光纤Bragg光栅在光纤激光器中的应用[J]. 激光与光电子学进展，2020，57(11)：111426.
Lü R D，Chen T，Fan C S，et al. Application of fiber lasers based on femtosecond laser inscribed fiber Bragg gratings[J]. Laser & Optoelectronics Progress，2020，57(11)：111426.

[21] 李宏业，武柏屹，王蒙，等. 飞秒激光刻写FBG实现3.2 kW单模光纤振荡器[J]. 中国激光，2022，49(3)：0315002.
Li H Y，Wu B Y，Wang M，et al. 3.2 kW single-mode fiber oscillator based on FBGs inscribed by femtosecond laser[J]. Chinese Journal of Lasers，2022，49(3)：0315002.

[22] 李宏业，田鑫，李昊，等. 飞秒激光刻写FBG实现5 kW近单模光纤振荡器[J]. 中国激光，2022，49(6)：0616001.
Li H Y，Tian X，Li H，et al. Realization of 5 kW near single mode fiber oscillator by femtosecond laser writing FBG[J]. Chinese Journal of Lasers，2022，49(6)：0616001.

[23] 李昊，叶新宇，王蒙，等. 飞秒激光刻写光纤布拉格光栅实现8 kW光纤振荡器[J]. 中国激光，2022，49(23)：2316001.
Li H，Ye X Y，Wang M，et al. Realization of 8 kW fiber oscillator by femtosecond laser writing fiber Bragg grating[J]. Chinese Journal of Lasers，2022，49(23)：2316001.

[24] Krämer R G，Möller F，Matzdorf C，et al. Extremely robust femtosecond written fiber Bragg gratings for an ytterbium-doped fiber oscillator with 5 kW output power[J]. Optics Letters，2020，45(6)：1447-1450.

[25] Li H Y，Tian X，Li H，et al. Fiber oscillator of 5 kW using fiber

Bragg gratings inscribed by a visible femtosecond laser[J]. Chinese Optics Letters, 2023, 21(2): 021404.
[26] Li H, Yang B L, Wang M, et al. Femtosecond laser fabrication of large-core fiber Bragg gratings for high-power fiber oscillators [J]. APL Photonics, 2023, 8(4): 046101.
[27] 李昊, 王蒙, 武柏屹, 等. 基于飞秒激光制备的啁啾倾斜布拉格光纤光栅[J]. 光学学报, 2023, 43(5): 0536001.
Li H, Wang M, Wu B Y, et al. Fabrication of chirped and tilted fiber Bragg gratings with femtosecond laser[J]. Acta Optica Sinica, 2023, 43(5): 0536001.
[28] Li H, Wang M, Wu B, et al. Femtosecond laser fabrication of chirped and tilted fiber Bragg gratings for stimulated Raman scattering suppression in kilowatt-level fiber lasers[J]. Optics Express, 2023, 31(8): 13393-13401.
[29] 李昊, 王蒙, 武柏屹, 等. 飞秒级联啁啾倾斜光纤光栅用于拉曼滤除[J]. 光学学报, 2023, 43(10): 1036001.
Li H, Wang M, Wu B Y, et al. Femtosecond cascade chirped and tilted fiber Bragg gratings for Raman filtering[J]. Acta Optica Sinica, 2023, 43(10): 1036001.
[30] Tao R M, Ma P F, Wang X L, et al. 1.3 kW monolithic linearly polarized single-mode master oscillator power amplifier and strategies for mitigating mode instabilities[J]. Photonics Research, 2015, 3(3): 86-93.
[31] Hejaz K, Shayganmanesh M, Rezaei-Nasirabad R, et al. Modal instability induced by stimulated Raman scattering in high-power Yb-doped fiber amplifiers[J]. Optics Letters, 2017, 42(24): 5274-5277.

High-Power Chirped and Tilted Fiber Gratings Written by Femtosecond Lasers

Li Hao[1,2], Ye Xinyu[1,2], Wang Meng[1,2,3*], Wu Baiyi[1,2,3], Gao Chenhui[1,2], Chen Zilun[1,2,3], Wang Zefeng[1,2,3**], Chen Jinbao[1,2,3]

[1]*College of Advanced Interdisciplinary Studies, National University of Defense Technology, Changsha* 410073, *Hunan, China*;
[2]*Nanhu Laser Laboratory, National University of Defense Technology, Changsha* 410073, *Hunan, China*;
[3]*Hunan Provincial Key Laboratory of High Energy Laser Technology, National University of Defense Technology, Changsha* 410073, *Hunan, China*

Abstract

Objective High-power fiber lasers are of application significance in scientific research and industrial processing. Stimulated Raman scattering (SRS) is a main factor limiting the power scaling of high-power fiber lasers. As a spectral filter component, chirped and tilted fiber Bragg grating (CTFBG) has been extensively studied to suppress SRS or filter Raman light in recent years. The traditional CTFBG fabrication method is the ultraviolet laser phase mask, but the fiber must be hydrogen-loaded and annealed before and after inscribing the grating, which leads to a long fabrication period. Additionally, if the annealing treatment is incomplete, the residual hydrogen molecules and hydroxyl compounds in the fiber would absorb near-infrared laser for heating to limit the power handling capability of CTFBG. To this end, the special annealing method, multiplexed inscribing technology, and efficient refrigeration packaging are proposed, but these methods and technologies greatly increase the fabrication period, cost, and complexity of high-power CTFBG. The development of femtosecond laser inscribing technology provides a new scheme for fabricating high-power CTFBG. As femtosecond lasers do not require the photosensitivity of the fiber, hydrogen loading, and annealing treatment are not needed, which shortens the fabrication period and avoids the heating caused by incomplete annealing. Meanwhile, since the fiber Bragg grating (FBG) written by femtosecond lasers feature high-temperature resistance, they have better tolerance to the temperature rise caused by a high-power laser.

Method Two FBGs and a CTFBG are inscribed in 20/400 μm large-mode-area double-cladding fiber by femtosecond laser phase mask method, as shown in Figs. 1 and 2. The central wavelengths of two FBGs are 1080 nm. The bandwidth and reflectivity of high reflective FBG (HRFBG) are 3.6 nm and more than 99% respectively, and those of low reflective FBG (LRFBG) are 1.2 nm and 10% respectively. The filtering band central wavelength of the CTFBG is 1133 nm with a 3 dB bandwidth of 17.3 nm and a filtering depth greater than 20 dB. The loss of CTFBG at 1080 nm signal power is less than 2% measured by the cut-off method. Two FBGs are employed to build a high-power fiber oscillator for testing CTFBG, and the CTFBG is inserted in the resonant cavity of the fiber oscillator, as shown in Fig. 3.

Results and Discussions Figs. 4, 5, and 6 show the CTFBG testing results based on the high-power fiber oscillator. When the CTFBG is not inserted, the output power does not increase after the pump power exceeds 3500 W due to transverse mode instability (TMI). At maximum pump power, the output power is 2678 W, corresponding to the optical-

to-optical conversion efficiency of 69.7% and the beam quality M^2 factor of 1.54. After inserting CTFBG into the resonant cavity, the SRS is suppressed with a Raman suppression ratio of ~13 dB, and the TMI is not observed. The maximum output power is increased to 2811 W, corresponding to the optical-to-optical conversion efficiency of 73.2%, and the beam quality M^2 factor is reduced to 1.43. During power scaling, the CTFBG is not packaged and cooled by a fan. The temperature slope of CTFBG is 7.9 ℃/kW, and the maximum temperature is 44 ℃。

Conclusions High-power CTFBG is inscribed in large-mode-area double-cladding fibers based on the femtosecond laser phase mask method. To test the power handling capability, the CTFBG is introduced into the resonant cavity of the high-power fiber oscillator. The maximum handling power of CTFBG is 2.8 kW, and the insertion loss of CTFBG is less than 2%. The CTFBG is cooled by an air fan during the test, and the temperature slope of CTFBG is 7.9 ℃/kW. This study shows that the femtosecond laser-written CTFBG has excellent power handling capability and temperature characteristics, which will promote the development and application of CTFBG. In the future, the CTFBG will be fabricated in larger core fibers by femtosecond lasers, and its performance will be further investigated in fiber lasers with higher output power.

Key words femtosecond lasers; fiber lasers; stimulated Raman scattering; fiber gratings; chirped and tilted fiber gratings